Available online at www.sciencedirect.com
SCIENCE DIRECT®
Journal of Molecular Catalysis A: Chemical 209 (2004) 199–207
JOURNAL OF MOLECULAR CATALYSIS A: CHEMICAL
www.elsevier.com/locate/molcata

The influence of surface acidity on NO_2 reduction by propane under lean conditions

Hanna Härelind Ingelsten [a,b], Åsa Hildesson [a,c], Erik Fridell [a,c], Magnus Skoglundh [a,b,*]

[a] *Competence Centre for Catalysis, Chalmers University of Technology, Kemigarden 3-4, Göteborg SE-412 96, Sweden*
[b] *Applied Surface Chemistry, Chalmers University of Technology, Kemigarden 3-4, Göteborg SE-412 96, Sweden*
[c] *Department of Applied Physics, Chalmers University of Technology, Kemigarden 3-4, Göteborg SE-412 96, Sweden*

Received 20 June 2003; accepted 26 August 2003

Abstract

This investigation focuses on the influence of surface acidity on the continuous catalytic reduction of NO_x by propane under lean conditions. The acidity was varied by studying noble metal free alumina, silica and co-precipitated aluminium-silicates with varying alumina–silica ratio. The catalysts were characterised by isopropylamine temperature programmed desorption (TPD), with respect to NO_x reduction (NO_2 and propane) and by Fourier Transform Infrared (FTIR) spectroscopy. The isopropylamine TPD was used to determine the sample acidity. The amount of Brønsted acid sites increased with increasing amount of alumina. The sample activity for NO_x reduction with propane was found to correlate with the Brønsted-site density. Furthermore, no N_2O was formed during the activity studies. The FTIR measurements implied formation of isocyanate species on the surface of the catalyst sample when NO/NO_2, propane and oxygen were present in the gas phase. FTIR data also reveal an increasing amount of adsorbates on the surface with increasing amount of alumina in the sample. Moreover, with propane present, NO-species were consumed to a higher extent over samples containing a larger amount of alumina. Our results suggest a connection between the Brønsted-site density and the NO_x reduction with propane under lean conditions.

Keywords: Aluminum-silicate; Lean NO_x reduction; Propane; Surface acidity; FTIR

1. Introduction

Combustion of fossil fuels, for instance originating from mobile sources, generates hazardous emissions such as NO_x, CO, unburned hydrocarbons and particulate matter. The traditional three way catalyst (TWC) can handle these pollutants satisfactory at stoichiometric conditions for petrol applications. In order to enhance the fuel economy, and hence reduce the CO_2 formation, it is desirable to use diesel or lean burn engines. However, the lean environment obstructs NO_x reduction utilising the TWC. This calls for the need of more efficient NO_x abatement techniques. During the last years several solutions have been introduced, e.g. NO_x storage [1,2] and selective catalytic reduction using ammonia (NH_3-SCR) [3] or hydrocarbons (HC-SCR) [4–11] as the reducing agent for NO_x.

For HC-SCR, catalysts based on Pt have been suggested as highly active towards NO reduction under lean conditions [12,13]. Unfortunately, the high activity is accompanied by low selectivity for N_2 formation [12], i.e. large quantities of N_2O are formed over Pt under lean conditions. However, by introduction of, e.g. acidic groups on the surface of the support material, the selectivity towards N_2 formation may be enhanced [14]. Furthermore, if the support material is modified for example to contain strong acidic sites [15,16] or by introduction of surface sulphates [17–22] it has been found that saturated hydrocarbons, such as propane, can be activated, i.e. some kind of carbonium ion is formed, on the surface of the support material. It has previously been reported [23,24] that Brønsted acid sites can be involved in alkane cracking. Furthermore, the Brønsted-site density of the catalyst surface probably also affects the NO_x reduction when saturated hydrocarbons are used as the reducing agent [25].

* Corresponding author. Tel.: +46-31-772-2974; fax: +46-31-16-00-62.
E-mail address: skoglund@surfchem.chalmers.se (M. Skoglundh).

1381-1169/$ – see front matter © 2003 Elsevier B.V. All rights reserved.
doi:10.1016/j.molcata.2003.08.016

Acke et al. [4,5] and Acke and Skoglundh [6–8] found that lean reduction of NO_x, by either C_3H_6, C_3H_8, NH_3 or HNCO, is affected by the platinum support material, i.e. γ-Al_2O_3, ZSM-5 or SiC, with respect to both the total NO_x conversion and the selectivity towards N_2. The lowest activity for NO_x reduction and the lowest selectivity towards N_2 formation was found for the samples supported on SiC. Acke and Skoglundh [8] also studied the lean NO reduction with propene and propane over unsupported platinum. Propene was found to reduce NO, whereas no reduction of NO was observed with propane. Thus, previous works show that the support material plays an important role for the lean NO reduction by propane and related hydrocarbons.

In a previous study [25], we investigated the lean NO reduction by propene and propane over Pt catalysts supported on alumina, silica and aluminium-silicates. That study indicated a strong connection between the amount of Brønsted acid sites in the sample and the selectivity towards N_2 formation, when propane was used as the reducing agent. Also the reduction of NO seemed to be influenced by the amount of Brønsted acid sites on the sample, using propane as the reductant. The NO reduction over supported Pt catalysts, by hydrocarbons, under lean conditions, has also been investigated by Burch et al. [9–11]. Using propene as the reducing agent, a mechanism was proposed where NO adsorbs dissociatively on vacant Pt sites to form N_2 or N_2O [9,10]. This is in accordance with Denton et al. [26], who concluded that propene protects the Pt surface from being oxygen poisoned and that oxygen, in turn, protects the Pt surface from carbonaceous deposits. When more weakly adsorbing reductants, e.g. propane, are used for the lean NO reduction [11], the nitric oxide is oxidised to NO_2 over the Pt surface. The NO_2 is then proposed to spill over from the platinum to the support material where it reacts with propane-derived species to form N_2 and N_2O [11].

This study focuses on the continuous catalytic reduction of NO_x by propane over alumina, silica and co-precipitated aluminium-silicates, in absence of precious metal, under lean (i.e. oxygen excess) conditions. The objective is to investigate the connection between the surface acidity of the samples and the activity of the NO_x reduction and the selectivity for N_2 formation.

2. Experimental procedure

2.1. Catalyst preparation

Three types of catalyst samples were investigated; alumina (Puralox NGa-180, Condea), silica (Bindzil 40-NH3-170, Akzo Nobel) and co-precipitated, calcined, hydrated aluminum-silicates (SIRAL, Condea) [27], with varying alumina–silica ratio (see Table 1). The aluminum-silicate samples most likely contain one or a combination of two or three phases at the surface; alumina, silica and/or aluminosilicate [27]. The latter phase is formed through isomorphous substitution of lattice Si^{4+} by Al^{3+} ions [27].

Table 1
Nominal composition and specific and total BET-surface area of the prepared samples

Sample	Sample composition Al_2O_3:SiO_2 (wt.%)	Specific surface area of the samples (m^2/g)	Total surface area of the washcoated monolith samples (m^2)
Al_2O_3	100:0	181	24.8
SIRAL1.5	98.5:1.5	279	24.9
SIRAL 20	80:20	405	24.8
SIRAL 40	60:40	503	24.5
SIRAL 70	30:70	441	25.9
SiO_2	0:100	148	26.1

The samples were calcined in air at 600 °C for 2 h, and the surface areas were then measured using nitrogen adsorption [28] according to the BET-method (see Table 1). During the calcination the hydrated aluminum-silicates were dehydrated and transformed to the corresponding aluminum-silicates. The as-prepared powders were used in the Fourier Transform Infrared (FTIR) spectroscopy measurements. For the flow reactor experiments, monolith substrates [25,28,29], were immersed in washcoat slurries containing the different support materials and 20 wt.% colloidal silica (Bindzil 40-NH3-170, Akzo Nobel), dispersed in distilled water (20 wt.% washcoat), according to a method described in detail previously [25]. The total surface area of the samples (25 m^2) and the monolith volume (1.79 cm^3) were kept constant.

2.2. Activity and characterisation

2.2.1. NO_x reduction activity

The activity and selectivity for NO_x reduction with C_3H_8 were investigated in a flow reactor, which is described in detail elsewhere [25,28]. Gases, Ar (99.998%), O_2 (99.95%), NO_2 (99.9%) and C_3H_8 (99.5%), were introduced via mass flow controllers (Bronkhorst Hi-tech) before the sample, and reactant and product gases were analysed on-line with respect to NO and NO_2 (CLD 700 EL ht, Chemiluminescense detector, TECAN), N_2O (UNOR 610, Infrared detector, Maihak), CO and CO_2 (UNOR 6N, Infrared detectors, Maihak) and total hydrocarbon content (VE 5, Flame ionisation detector, J.U.M. Engineering). To investigate if other products were formed, a gas phase FTIR (Excalibur Series, Bio-Rad, FTS3000MX with liquid nitrogen cooled MCT detector and Specac gas cell with 2 m path length) was used during steady-state measurements at 650, 600, 550, 500 and 450 °C, this set of data was performed after the ramp experiments.

The gas composition used in the experiments was; 3% O_2, 380 ppm NO_2 and 1800 ppm C_3H_8, balanced with Ar to maintain a total gas flow rate of 1500 ml/min, corresponding to a space velocity of 50000 h^{-1}. The samples were initially conditioned in the reaction gas mixture at 650 °C for 30 min. Cooling and heating ramp experiments (650 °C →

200 °C → 650 °C) were subsequently carried out with a constant ramp rate of 10 °C/min.

2.2.2. Isopropylamine temperature programmed desorption (TPD)

To determine the acidity of the samples, isopropylamine TPD experiments were performed in a second flow reactor, described elsewhere [25,30]. The gases, H_2 (99.995%), O_2 (99.95%), Ar (99.9997%) and Ar (99.9997%) saturated with isopropylamine (Merck, >99%), were introduced, via mass flow controllers (Brooks 5850S), before the sample and the gas composition after the sample was probed using a quartz capillary and continuously measured by a quadrupole mass spectrometer (Balzers QMS 200). The analysed *m*/*e* ratios were: 2 (H_2), 17 (NH_3 and isopropylamine), 32 (O_2), 40 (Ar), 41 (propene and isopropylamine) and 44 (isopropylamine).

The samples were first pre-oxidised with 10% O_2 in Ar (400 °C, 15 min, 200 ml/min) and then pre-reduced with 1% H_2 in Ar (400 °C, 15 min, 200 ml/min). The samples were subsequently exposed to isopropylamine (2% in Ar, 200 ml/min) at 25 °C until saturation was reached (about 5 min) [25]. After the isopropylamine exposure the system was exposed to pure Ar for one hour in order to evacuate isopropylamine adsorbed on the equipment, and the TPD experiment (25 °C → 550 °C, 20 °C/min) was performed under Ar (at a total flow rate of 200 ml/min).

2.2.3. FTIR spectroscopy

The in situ FTIR spectroscopy measurements were carried out using a BioRad FTS 6000 spectrometer in diffuse reflectance (DRIFT) mode. The set-up is described elsewhere [31]. The powder samples were ground and diluted (1:5) in KBr and about 30 mg was placed in the DRIFT cell. The gases, Ar (99.995%), H_2 (99.995%), O_2 (99.95%), NO (99.9%), NO_2 (99.9%) and C_3H_8 (99.5%), were introduced via mass flow controllers (Bronkhorst Hi-Tech) to the DRIFT cell.

The samples were initially pre-treated in oxygen (10% O_2 in Ar, 550 °C, 15 min) followed by hydrogen (1% H_2 in Ar, 550 °C, 15 min) and finally in oxygen (same as previously) at a total flow rate of 300 ml/min (the flow rate was kept constant throughout the experiment). The sample cell was then flushed with pure Ar during 15 min and background spectra (100 scans at a resolution of 1 cm^{-1} at each temperature) were collected under Ar exposure at 500, 400, 300 and 200 °C, respectively. Steady-state measurements (40 scans at a resolution of 1 cm^{-1}) were subsequently performed at 500, 400, 300 and 200 °C with different gas compositions: (i) 400 ppm NO, 400 ppm NO_2 and 3% O_2, (ii) 500 ppm C_3H_8 and 3% O_2 and (iii) 400 ppm NO, 400 ppm NO_2, 500 ppm C_3H_8 and 3% O_2. All mixtures were diluted with Ar to obtain a total flow rate of 300 ml/min. Between the different gas compositions the pre-treatment was repeated and new background spectra were collected.

3. Results and discussion

3.1. Activity studies

The results from the NO_x reduction experiments with NO_2, C_3H_8 and O_2 are summarised in Tables 2 and 3. The result for the Al_2O_3 sample is shown in Fig. 1, where the outlet concentrations of NO_x ($NO + NO_2$), NO, NO_2, N_2O, CO and CO_2 are plotted versus the catalyst inlet temperature. The inlet concentration of NO_2 was about 380 ppm, hence, divergence from this value in the NO_x signal should be due to adsorption–desorption of NO, NO_2 or N_2O and/or formation of N_2.

The Al_2O_3 sample reached the highest NO_x reduction of all samples investigated (see Fig. 2 and Table 2). The NO_x reduction decreased with increasing silica content in the samples and the SIRAL40, the SIRAL70 and the SiO_2 samples all showed low NO_x reduction. The maximum NO_x reduction was obtained around 550 °C for the Al_2O_3, the SIRAL1.5 and the SIRAL20 samples, whereas the SIRAL40, the SIRAL70 and the SiO_2 samples showed their highest reduction (a few percent) at the highest temperature studied, 650 °C. Furthermore, we have performed NO_x reduction experiments over the Al_2O_3 sample using different amounts of propane (where the NO_2:C_3H_8 molar ratio was 1:3, 1:4 and 1:6, respectively). Since approximately the same NO_x reduction was obtained, as with the lower concentrations the reduction seems to be insensitive to the C_3H_8 concentration. Experiments were also performed with

Table 2
Maximum NO_x reduction and the corresponding temperature during cooling and heating ramps

Sample	NO_x reduction, cooling ramp (%)	Corresponding temp. (°C)	NO_x reduction, heating ramp (%)	Corresponding temp. (°C)	Specific activity at 500 °C (mol/(m^2 s))
Al_2O_3	19	538	20	551	2.2×10^{-9}
SIRAL1.5	14	549	15	552	1.4×10^{-9}
SIRAL 20	8.0	547	8.5	562	7.0×10^{-10}
SIRAL 40	3.6	650[a]	4.2	650[a]	1.9×10^{-10}
SIRAL 70	3.0	650[a]	3.1	650[a]	1.5×10^{-11}
SiO_2	3.1	650[a]	3.2	650[a]	2.9×10^{-11}

Also included is the specific activity for NO_x reduction at 500°C (cooling ramp).
[a] Highest temperature.

Table 3
C_3H_8 conversion, CO_2 formation, T_{50,CO_2} (temperature where 50% of the species is formed), CO formation and $T_{50,CO}$ during cooling ramps

Sample	Maximum C_3H_8 conversion	CO_2 formation start (°C)	T_{50,CO_2} (°C)	Maximum CO_2 formation (ppm)	CO formation start (°C)	$T_{50,CO}$ (°C)	Maximum CO formation (ppm)
Al_2O_3	18	335	516	824	379	582	514
SIRAL1.5	11	345	530	389	377	550	362
SIRAL 20	7.3	340	552	310	370	595	311
SIRAL 40	6.3	365	573	151	425	624	146
SIRAL 70	6.9	390	579	103	450	633	114
SiO_2	6.8	430	596	74	495	639	163

NO and propane and with a mixture of 66% NO and 33% NO_2 with propane over the alumina sample (see Fig. 3). These experiments indicated that the NO_x reduction was negligible when NO and propane was used, whereas the NO_x reduction for NO + NO_2 + propane was about half the value that was achieved for NO_2 + propane. From Table 3 it is evident that the propane oxidation was not complete for any of the samples investigated. However, the largest propane oxidation was obtained for the alumina sample and the propane oxidation was then decreasing with increasing silica content in the sample.

As can be seen in Fig. 1, the N_2O signal, for the Al_2O_3 sample, was approximately zero at low temperature, increased slowly as the temperature was raised and reached 4 ppm at about 650 °C. This result was similar for all samples investigated, and since from thermodynamic considerations we do not expect N_2O to be formed at 650 °C, we believe that this signal was due to interference with water, i.e. formed during the oxidation of propane. The product gases were also analysed by gas phase FTIR in order to detect nitrogen containing species other than NO, NO_2 and N_2O such as HCN, HNCO and NH_3, which have been reported as intermediate species during lean NO_x reduction by hydrocarbons [4,5,32–34]. The results were similar for all samples and the quantitative spectra show the expected NO (absorption bands at 1897 and 1857 cm^{-1}), NO_2 (1594 cm^{-1}), propane (2968, 1468 cm^{-1}), propene (2968, 1632, 1468, 912 cm^{-1}), CO (2159, 2124 cm^{-1}) and CO_2 (2359 cm^{-1}). We observed a small peak at 712 cm^{-1}, however we can not attribute this peak to HCN [34] since no peak was observed at 3311 cm^{-1}. We also observed small peaks at 950, 922 and 1632 cm^{-1} which could not be assigned to NH_3 [34] since the expected peak at 3338 cm^{-1} was not observed. From these results one may conclude that the major reduction product, during these experiments, was N_2 since only small peaks that might correspond to HCN and NH_3 were observed and no signatures of N_2O were found.

In order to investigate if the catalytic activity of the samples was limited by mass transport of reactants, the Weiszs-modulus for the reactions at 500 °C was estimated. Mass transport limitations become important when the Weiszs-modulus, Φ, has a value of approximately one or higher [35]. The Weiszs-modulus is given by:

$$\Phi = \frac{L^2 r}{D_{\text{eff}} c_{\text{as}}} \quad (1)$$

where L is the thickness of the washcoat layer, r the reaction rate, D_{eff} the effective diffusivity and c_{as} the surface

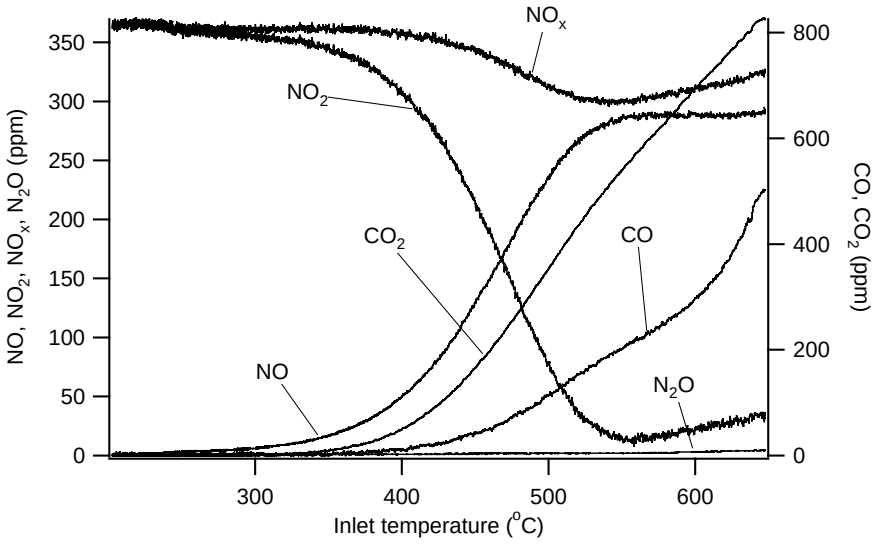

Fig. 1. NO_2 conversion with propane over the Al_2O_3 sample during lean conditions (cooling ramp).

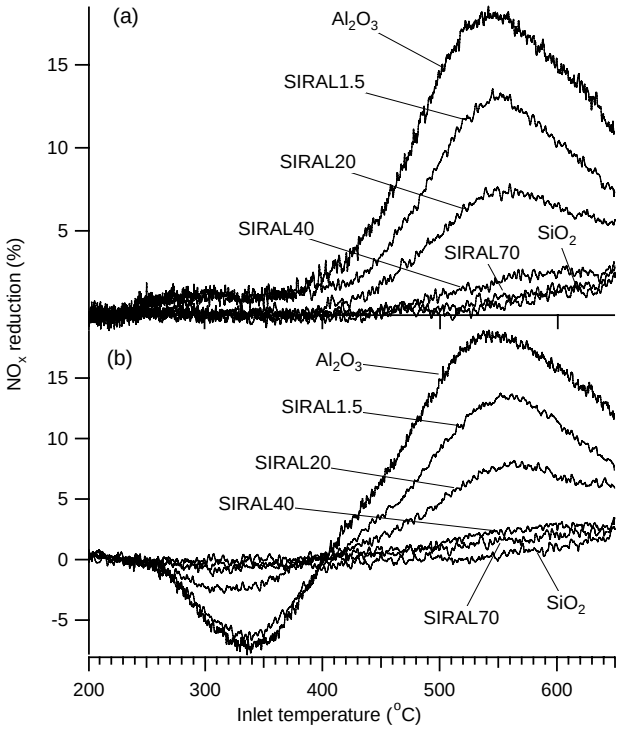

Fig. 2. NO_x reduction (%) during (a) cooling ramp and (b) heating ramp.

concentration of the reactant (i.e. NO_2). At 500 °C the Weiszs-modulus were calculated to 0.8 for Al_2O_3, 0.7 for SIRAL1.5, 0.5 for SIRAL20, 0.2 for SIRAL40 and 0.01 for SIRAL70 and SiO_2, respectively. Hence, it is reasonable to assume that the catalytic reaction was not influenced by mass transport limitations. (In Table 2 the specific activities at 500 °C are listed.)

3.2. Acidity measurements

The acidity of a solid sample can be investigated using TPD of isopropylamine (C_3H_9N). With this method it is possible to determine the density of Brønsted acid sites since the isopropylamine is decomposed over this type of site, in a narrow temperature range forming propene and ammonia [23,24,36,37]. The reaction over the Brønsted-site is similar to the Hofmann elimination [38]:

$$HRNH_2 + MOH \rightarrow HRNH_3^+ + MO^-$$

$$HRNH_3^+ + MO^- \rightarrow R + NH_3 + MOH$$

where M represents the surface of the support material and R the hydrocarbon chain.

The results from the isopropylamine TPD experiments are summarised in Table 4 and Fig. 4. Unreacted isopropylamine desorbed from the samples below 250 °C with a maximum desorption at about 100 °C for all samples. The highest amount of desorbed isopropylamine was found for the SiO_2 sample. The SIRAL70 sample showed the lowest amount of desorbed unreacted isopropylamine (see Table 4 and Fig. 4a). Desorption of unreacted isopropylamine can be attributed to Lewis acid sites [24,36] at the surface of the sample. At higher temperatures (between 300 and 450 °C), formation of propene and ammonia were observed (maximum formation at about 375 and 380 °C, respectively), and, as can be seen from Table 4, the propene formation seemed to be lower than the formation of ammonia probably due to influence from water on *m/e* 17. The Al_2O_3, SIRAL1.5 and SIRAL20 samples showed the largest formation of propene and ammonia. However, the amount of formed propene and ammonia decreased with increasing amount of SiO_2 in the sample, i.e. the formation decreased in the order $Al_2O_3 \geq$ SIRAL1.5 $\geq$ SIRAL20 $>$ SIRAL40 $>$ SIRAL70 $>$ SiO_2 (see Table 4 and Figs. 4b and c). The SiO_2 sample did not show any propene or ammonia formation at all. Formation of ammonia and propene occurs when isopropylamine is decomposed over Brønsted acid sites [23,24,36,37]. Since the ammonia and propene formation decreased as the silica content in the samples increased it seems reasonable to assume that the amount of Brønsted acid sites in the samples most likely decreases in the order $Al_2O_3 \geq$ SIRAL1.5 $\geq$ SIRAL20 $>$ SIRAL40 $>$ SIRAL70 $>$ SiO_2, i.e. the Al_2O_3 sample contains the highest amount of Brønsted acid sites, whereas the SiO_2 sample does not contain any Brønsted acid sites, since no propene and ammonia was formed over this sample (see Fig. 5).

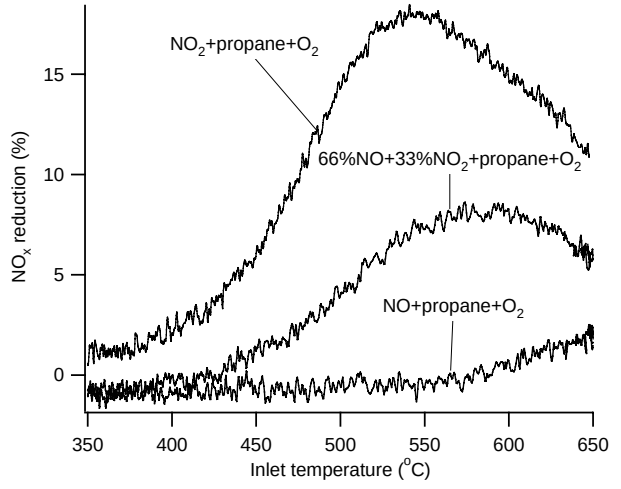

Fig. 3. NO_x reduction (%) using different NO_x sources: NO_2, 66% NO + 33% NO_2 and NO, respectively, with propane over the Al_2O_3 sample (cooling ramp).

3.3. Surface adsorbates

Knözinger and Ratnasamy [39] proposed to investigate alumina surface structure by measuring the OH stretching vibrations. Usually alumina gives rise to three main bands in the region 3700–3800 cm^{-1}, but with sufficiently high resolution five bands can be observed. Knözinger and Ratnasamy attribute these five bands to different OH configurations on the alumina surface. Since the OH groups in these various configurations have slightly different net charges, they should possess different properties, for instance

Table 4
Isopropylamine (C_3H_9N) desorption (des.), propene and ammonia formation and temperatures at maximum desorption or formation during isopropylamine TPD

Sample	C_3H_9N des. (μmol)	C_3H_9N des. (°C)	C_3H_6 formation (μmol)	C_3H_6 formation (°C)	NH_3 formation (μmol)	NH_3 formation (°C)
Al_2O_3	4.7	102	11.4	376	19	374
SIRAL 1.5	4.6	101	10.8	372	18	378
SIRAL 20	4.0	96	10.8	374	13	383
SIRAL 40	3.1	96	9.4	370	10	383
SIRAL 70	2.6	100	8.3	372	9	381
SiO_2	5.7	107	–	–	–	–

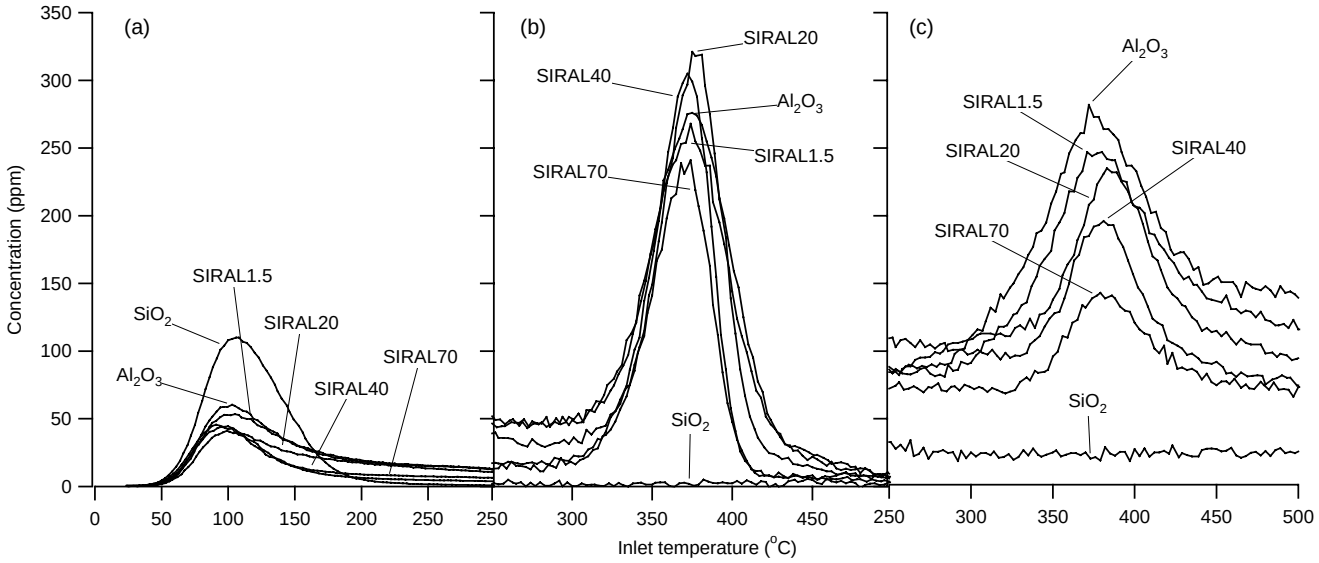

Fig. 4. Isopropylamine TPD experiments. (a) isopropylamine desorption (ppm), (b) propene formation (ppm) and (c) ammonia formation (ppm).

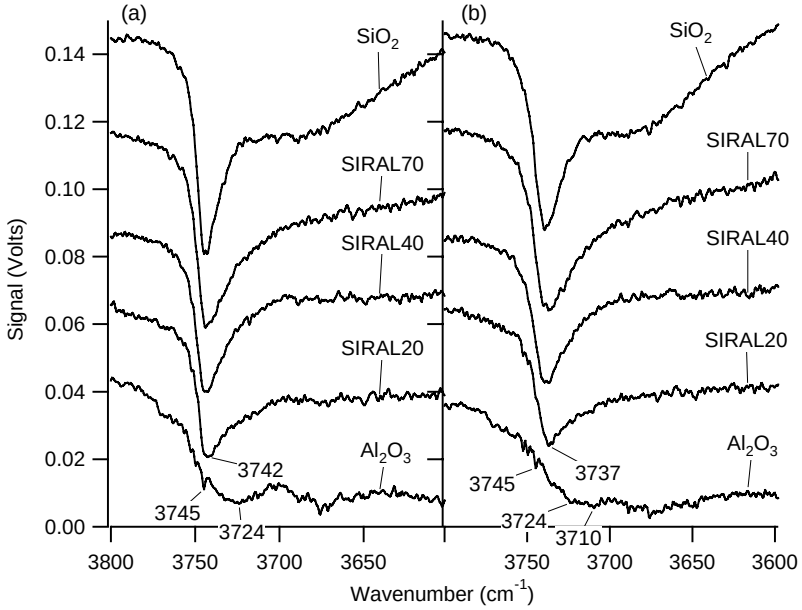

Fig. 5. FTIR spectra collected at steady-state during Ar flow at (a) 200 °C and (b) 500 °C. The baselines are separated by 0.02.

different acidity [39]. Figs. 5a and b show the background IR spectra for the samples, after the pre-treatment, at 200 and 500 °C, respectively. A sharp negative absorption peak was observed at 3742–3745 cm^{-1} (200 °C) and at 3737–3745 cm^{-1} (500 °C), for all samples. Covalently bonded oxides, like silica, show strong sharp absorption peaks originating from OH stretching vibrations, which, for silica, occurs in the region 3750–3730 cm^{-1} [40]. For the alumina containing samples peaks in this region can most probably be assigned to a configuration which Knözinger and Ratnasamy [39] designate Type IIb (3740–3745 cm^{-1}), where the OH-group is linked to two Al-cations in octahedral positions. As the silica content increased, i.e. the samples were more silica-like [27], the peak in this region became more narrow, in accordance with Busca [40] and Daniell et al. [27]. At 200 °C, the Al_2O_3 sample showed a small peak at 3745 cm^{-1} and a broad peak centred around 3724 cm^{-1}. The spectrum for the Al_2O_3 sample at 500 °C was similar, however, an additional peak centred around 3710 cm^{-1} became visible. The peak centred at 3710 cm^{-1} is likely to be attributed to the Type III (3700–3710 cm^{-1}) configuration with an OH-group bonded to three Al-cations in octahedral positions [39]. This type of configuration is expected to be the most acidic one having a net positive charge estimated to +0.5 [39]. The other peak, centred around 3724 cm^{-1}, can supposedly be ascribed to either Type III or Type IIa (3730–3735 cm^{-1}), where the latter one is an OH-group linked to one Al-cation in octahedral position and one in tetrahedral position. This result, together with the result from the isopropylamine TPD, indicates that the surface of the alumina sample contains a higher density of more acidic Brønsted OH sites. Further, for the aluminium-silicate samples the Type IIb peak was broadened towards the Type III region as the alumina content in the samples increased. This indicate a Type III configuration for some of the OH-groups in these samples, hence, the aluminium-silicate samples may also possess the more acidic type of configuration.

During the steady-state measurements with $NO/NO_2 + O_2$, four main peaks in the region 1300–1650 cm^{-1} could be observed for the Al_2O_3 sample at 200 °C. These peaks gradually disappeared as the temperature and the silica content in the samples increased (see Fig. 6). These peaks can most likely be attributed to a mixture of monodentate nitrate, bidentate nitrate and bridged nitrate species [41,42] at the surface of the samples. One could also observe a broad band in the region 3400–3800 cm^{-1}, with a sharp negative peak around 3740 cm^{-1} and a broad positive band at lower frequency. The broad positive band occurred for all samples, except for the SiO_2 sample, at 200 °C, for the Al_2O_3 and SIRAL20 samples at 300 °C and was visible only for the Al_2O_3 sample at 400 °C, whereas the negative peak only occurred for the Al_2O_3 (200, 300 and 400 °C) and the SIRAL20 (200 and 300 °C) samples. The OH stretching mode is in this region, 3000–3800 cm^{-1} [40], and, as discussed previously, OH-groups were initially present

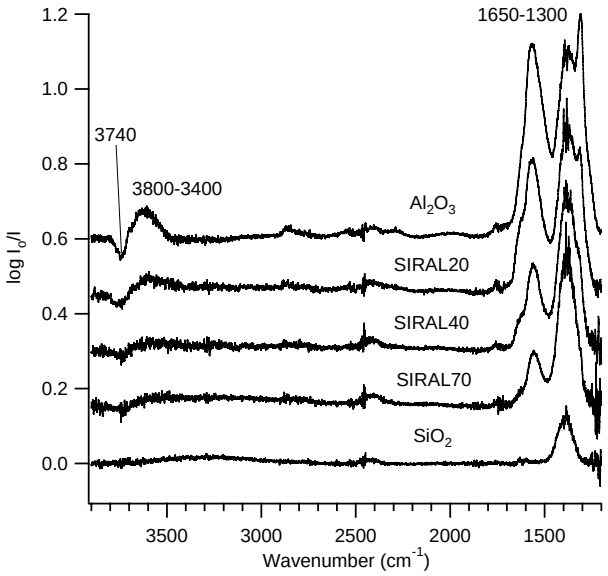

Fig. 6. FTIR spectra collected at steady-state during a flow of 400 ppm NO, 400 ppm NO_2 and 3% O_2 at 200 °C. The baselines are separated by 0.15.

at the surface of the samples. Hence, the sharp negative peak (around 3740 cm^{-1}) was likely to arise from blocking and/or disappearance of OH-groups at the surface, while the broad positive peak probably was due to adsorbates on the OH-groups thus causing a change in the OH stretching vibration frequency [40].

Three main peaks could be observed in the region 1200–1650 cm^{-1} during the $C_3H_8 + O_2$ steady-state measurements for the Al_2O_3 sample at 200 °C. Similarly as with $NO/NO_2 + O_2$ these peaks gradually disappeared as the temperature and silica content in the samples increased. In this region peaks have previously been assigned to surface bound formate [42–45], acetate [42,43,45], bidentate carbonate [46] and bicarbonate [46,47] species. It is, thus, likely that the peaks observed in this region could be assigned to combinations of surface carboxylates and surface carbonates. At 500 °C a peak around 2240 cm^{-1} was observed for the SIRAL40 sample (see Fig. 7b). In this region isocyanate (–NCO) species have been found [4,5,32,33,42,48,49]. As no nitrogen containing species were present in the feed during this experiment one may assume that the surface was not completely cleaned from nitrate species from the previous experiment, and hence –NCO species could be formed.

When performing the steady-state measurements with $C_3H_8 + NO/NO_2 + O_2$ several peaks in the range 1200–1800 cm^{-1} and a broad band in the range 2600–3800 cm^{-1} occurred. The overall impression was similar to the previously described results with a decreasing amount of adsorbates on the surface as the temperature and silica content in the samples increased. As mentioned before, peaks in the area 1200–1800 cm^{-1} can most probably be ascribed to a combination of monodentate nitrate, biden-

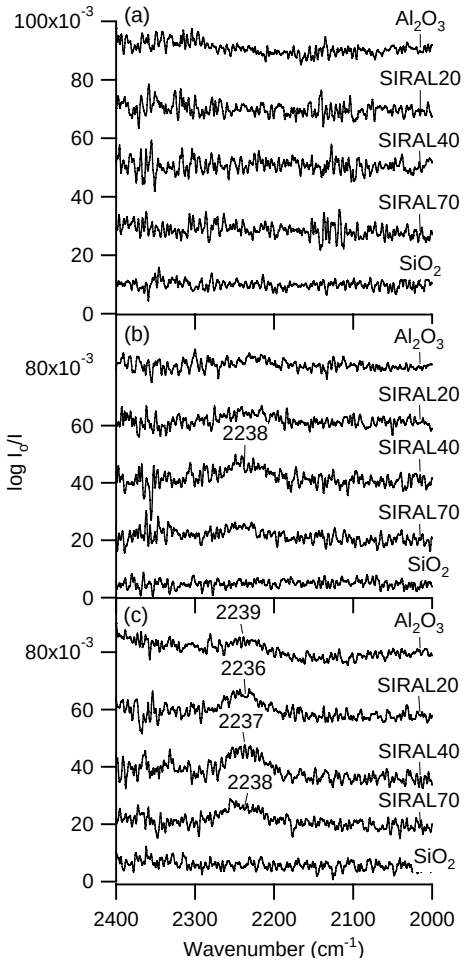

Fig. 7. FTIR spectra collected at 500 °C (steady-state) during a flow of (a) 400 ppm NO, 400 ppm NO_2 and 3% O_2, (b) 500 ppm C_3H_8 and 3% O_2, and (c) 400 ppm NO, 400 ppm NO_2, 500 ppm C_3H_8 and 3% O_2. The baselines are separated by 0.015.

tate nitrate and bridged nitrate [41,42] and/or surface carbonates and carboxylates [42–47]. The broad band in the range 2600–3800 cm^{-1} is probably related to surface OH groups, which occur in the region 3000–3800 cm^{-1} [40]. For the steady-state experiments with $C_3H_8 + NO/NO_2 + O_2$ a peak was found in the region 2230–2240, which was present for all samples except for the silica sample (see Fig. 7c). Peaks in this region have previously been assigned to surface isocyanate (–NCO) species [4,5,32,33,42,48,49].

From Fig. 7, it can be seen that no peaks in the isocyanate region (2230–2240 cm^{-1}) were observed for the experiment with $NO/NO_2 + O_2$ and only minor peaks were recorded for $C_3H_8 + O_2$. In the latter case, it is reasonable to assume that some nitrate species were still present on the surface since the experiment with nitrogen oxides was performed prior to the experiment with propane. The peaks were more intense for the experiments with NO/NO_2, propane and oxygen (compared to propane and oxygen) and could be observed for all samples except for the silica one. Hence, it seems likely that isocyanate species are formed on the surface of the sample in presence of both NO/NO_2 and propane. It has been debated in the literature whether isocyanate is an intermediate in the HC-SCR reaction or not [4,5,32,33,42]. From the experiments presented in this study it seems at least to be a connection between the NO_x reduction, the density of acidic Brønsted OH surface sites, the OH configuration on alumina and/or silica and the presence of isocyanate species on the surface. It is also worth noticing that in all FTIR experiments the amount of adsorbates, both N- and C-containing species and OH-groups, increased with increasing alumina content in the samples. Furthermore, it is likely that the OH-groups at the surface of the alumina and aluminium-silicate samples participated in the reactions since the IR vibration frequencies indicated adsorbates on the OH-groups. These adsorbates seemed to be present to a larger extent for the samples containing more alumina.

4. Concluding remarks

During the NO_x reduction experiments with propane it was found that the Al_2O_3 sample exhibited the highest NO_x reduction activity and that the activity decreased as the silica content in the samples increased. Although the activity was found to be lower over the pure support materials, than for the corresponding Pt-containing samples [25], this study undoubtedly shows that there is a clear correlation between the activity for NO_x reduction and the alumina content, i.e. the Brønsted-site density. During the experiments only small or negligible amounts of N_2O, HCN and NH_3 were formed, which demonstrates a high selectivity for N_2 formation in these experiments. For NO_x reduction by propane over Pt/alumina and Pt/aluminium-silicate samples, we have previously found [25] that the N_2 selectivity is strongly connected to the Brønsted-site density. Accordingly, it is reasonable to assume that N_2O preferably is formed over Pt sites. However, the amount of Brønsted sites on the support material seems to influence the ratio between N_2 and N_2O.

In the FTIR measurements, we observe a correlation between the amount of adsorbates (N- and C-containing species as well as OH-groups) and the amount of alumina. Further, it seemed as the nitrate species on the surface were consumed when propane was present, and the consumption seemed to increase with a larger amount of alumina in the samples, i.e. increasing consumption of nitrate species in the presence of propane as the Brønsted-site density increased. Also, for the alumina and aluminium-silicate samples, isocyanate species were found on the sample surface when both NO_x and propane was present in the gas phase.

To summarise, a close connection between the Brønsted-site density, the amount of adsorbates on the sample surface, the consumption of nitrate species in the presence of propane and most importantly the NO_x reduction has been demonstrated. Moreover, a connection to the surface isocyanate species was observed even though the correlation to the Brønsted-site density is not as clear. From this study it

is possible to conclude that even in the absence of precious metals, there is a reaction between NO_2 and C_3H_8 forming N_2 and CO_2 over alumina and aluminium-silicate samples and the activity is correlated to the alumina content in the samples, i.e. to the Brønsted-site density.

Acknowledgements

The authors would like to thank Condea for providing the support materials. This work has been performed within the Competence Centre for Catalysis, which is hosted by Chalmers University of Technology and financially supported by the Swedish Energy Agency and the member companies: AB Volvo, Johnson Matthey-CSD, Saab Automobile Powertrain AB, Perstorp AB, AVL-MTC AB, Akzo Nobel Catalysts BV and The Swedish Space Agency.

References

[1] N. Takahashi, H. Shinjoh, T. Iijima, T. Suzuki, K. Yamazaki, K. Yokota, H. Suzuki, N. Miyoshi, S. Matsumoto, T. Tanizawa, T. Tanaka, S. Tateishi, K. Kasahara, Catal. Today 27 (1996) 63.
[2] E. Fridell, M. Skoglundh, B. Westerberg, S. Johansson, G. Smedler, J. Catal. 183 (1999) 196.
[3] V.I. Parvulescu, P. Grange, B. Delmon, Catal. Today 46 (1998) 233.
[4] F. Acke, B. Westerberg, L. Eriksson, S. Johansson, M. Skoglundh, E. Fridell, G. Smedler, Stud. Surf. Sci. Catal. 116 (1998) 285.
[5] F. Acke, B. Westerberg, M. Skoglundh, J. Catal. 179 (1998) 528.
[6] F. Acke, M. Skoglundh, Appl. Catal. B 20 (1999) 133.
[7] F. Acke, M. Skoglundh, Appl. Catal. B 20 (1999) 235.
[8] F. Acke, M. Skoglundh, Appl. Catal. B 22 (1999) L1.
[9] R. Burch, A.A. Shestov, J.A. Sullivan, J. Catal. 182 (1999) 497.
[10] R. Burch, J.A. Sullivan, J. Catal. 182 (1999) 489.
[11] R. Burch, T.C. Watling, J. Catal. 169 (1997) 45.
[12] R. Burch, P.J. Millington, Catal. Today 26 (1995) 185.
[13] H. Hamada, Catal. Today 22 (1994) 21.
[14] G. Zhang, T. Yamaguchi, H. Kawakami, T. Suzuki, Appl. Catal. B 1 (1992) L15.
[15] H. Hattori, O. Takahashi, M. Takagi, K. Tanabe, J. Catal. 68 (1981) 132.
[16] M. Hino, K. Arata, Catal. Lett. 30 (1995) 25.
[17] R. Burch, E. Halpin, M. Hayes, K. Ruth, J.A. Sullivan, Appl. Catal. B 19 (1998) 199.
[18] C.P. Hubbard, K. Otto, H.S. Gandhi, K.Y.S. Ng, Catal. Lett. 30 (1995) 41.
[19] A.F. Lee, K. Wilson, R.M. Lambert, C.P. Hubbard, R.G. Hurley, R.W. McCabe, H.S. Gandhi, J. Catal. 184 (1999) 491.
[20] M. Skoglundh, A. Ljungqvist, M. Petersson, E. Fridell, N. Cruise, O. Augustsson, E. Jobson, Appl. Catal. B 30 (2001) 315.
[21] K. Wilson, C. Hardacre, R.M. Lambert, J. Phys. Chem. 99 (1995) 13755.
[22] H.C. Yao, H.K. Stephen, H.S. Gandhi, J. Catal. 67 (1981) 231.
[23] W.E. Farneth, R.J. Gorte, Chem. Rev. 95 (1995) 615.
[24] J.G. Tittensor, R.J. Gorte, D.M. Chapman, J. Catal. 138 (1992) 714.
[25] H.H. Ingelsten, M. Skoglundh, E. Fridell, Appl. Catal. B 41 (2003) 287.
[26] P. Denton, A. Giroir-Fendler, Y. Schuurman, H. Praliaud, C. Mirodatos, M. Primet, Appl. Catal. A 220 (2001) 141.
[27] W. Daniell, U. Schubert, R. Glockler, A. Meyer, K. Noweck, H. Knözinger, Appl. Catal. A 196 (2000) 247.
[28] M. Skoglundh, H. Johansson, L. Löwendahl, K. Jansson, L. Dahl, B. Hirschauer, Appl. Catal. B 7 (1996) 299.
[29] I.M. Axelsson, L. Löwendahl, J.E. Otterstedt, Appl. Catal. 44 (1988) 251.
[30] J. Jansson, J. Catal. 194 (2000) 55.
[31] A. Hinz, M. Skoglundh, E. Fridell, A. Andersson, J. Catal. 201 (2001) 247.
[32] G.R. Bamwenda, A. Ogata, A. Obuchi, J. Oi, K. Mizuno, J. Skrzypek, Appl. Catal. B 6 (1995) 311.
[33] Y.J. Mergler, B.E. Nieuwenhuys, J. Catal. 161 (1996) 292.
[34] F. Radtke, R.A. Koppel, A. Baiker, Catal. Today 26 (1995) 159.
[35] P.B. Weiszs, C.D. Prater, Adv. Catal. 6 (1954) 143.
[36] R.J. Gorte, Catal. Lett. 62 (1999) 1.
[37] O. Kresnawahjuesa, R. Heussner, C.C. Lee, G. Kuehl, R.J. Gorte, Appl. Catal. A 199 (2000) 53.
[38] A.W. Hofmann, Ann. Chem. Pharm. 78 (1851) 253.
[39] H. Knözinger, P. Ratnasamy, Catal. Rev. -Sci. Eng. 17 (1978) 31.
[40] G. Busca, Phys. Chem. Chem. Phys. 1 (1999) 723.
[41] B. Westerberg, E. Fridell, J. Mol. Catal. A 165 (2001) 249.
[42] D.K. Captain, M.D. Amiridis, J. Catal. 184 (1999) 377.
[43] V. Ermini, E. Finocchio, S. Sechi, G. Busca, S. Rossini, Appl. Catal. A 190 (2000) 157.
[44] D.G. Rethwisch, J.A. Dumesic, Langmuir 2 (1986) 73.
[45] K. Shimizu, H. Kawabata, A. Satsuma, T. Hattori, J. Phys. Chem. B 103 (1999) 5240.
[46] N.D. Parkyns, J. Phys. Chem. 75 (1971) 526.
[47] C. Morterra, G. Magnacca, Catal. Today 27 (1996) 497.
[48] F. Solymosi, L. Volgyesi, J. Sarkany, J. Catal. 54 (1978) 336.
[49] M.L. Unland, J. Phys. Chem. 77 (1973) 1952.